

## Optimization of Inner Bilge Design to Enhance Cargo Tank Capacity in Tankers

Ardi Nugroho Yulianto<sup>1\*</sup>, Raybonda Reinaldi Winarko<sup>1</sup>, Sheely Leony Artha Pasaribu<sup>1</sup>, Roisul Fadli Ahmad<sup>1</sup>, Berlian Arswendo Adietya<sup>2</sup>, Hasanudin<sup>1</sup>



<sup>1</sup>Department of Naval Architecture, Sepuluh Nopember Institute of Technology, Surabaya 60111, Indonesia

<sup>2</sup>Department of Naval Architecture, Diponegoro University, Semarang 50275, Indonesia Indonesia

<sup>\*</sup>Corresponding Author: [ardi.nugroho@its.ac.id](mailto:ardi.nugroho@its.ac.id)

### Article Info

### Abstract

#### Keywords:

Grid Search Method;  
Inner Bilge;  
Optimization;  
Tanker;  
Visual Basic for Application

#### Article history:

Received: 24/02/2026  
Last revised: 24/04/2026  
Accepted: 25/04/2026  
Available online: 25/04/2026  
Published: 30/04/2026

#### DOI:

<https://doi.org/10.14710/kapal.v23i1.82683>

The world of shipping industry keeps evolving to develop the most efficient ship designs, including tanker ship designs. According to MARPOL Annex 1 Regulation 19, oil tankers over 600 deadweight and built after 6 July 1996 must have wing tank and double bottom structures, which significantly reduce the cargo hold volume. Therefore, the objective of this research is to optimize the cargo hold volume by converting the conventional sloped hopper into a rounded inner bilge configuration. The optimization problem is formulated with the cargo oil tank volume as the objective function to be maximized. The design variables include the inner bilge radius and the positions of two cargo landing points at each knuckle along the cargo oil tank, defined in transverse and vertical coordinates. The constraints consist of regulatory and design requirements, including clearance, stability, freeboard, and longitudinal strength. Grid search method is employed to systematically evaluate all possible combinations of design variables, ensuring identification of the global optimum. The optimisation process is automated using Visual Basic for Applications (VBA) integrated with ship modelling software. The research resulted in a new design that increased the cargo oil tank volume by 0.960%. A sister ship with the same payload could be built with an optimized cargo oil tank design configuration by reducing the length of the cargo oil tanks and the ship itself. However, this improvement comes with a trade-off in terms of practical applicability during the shipbuilding process.

Copyright © 2026 KAPAL: Jurnal Ilmu Pengetahuan dan Teknologi Kelautan. This is an open access article under the CC BY-SA license (<https://creativecommons.org/licenses/by-sa/4.0/>).

## 1. Introduction

The world of shipping industry keeps evolving to develop the most efficient ship designs. Welding was started to be used in the 1930s to replace riveting method for joining ship hull because it was significantly reduced the ship lightweight. Some researchers have developed a new kind of material that is stronger but lighter than mild steel. Some have designed ship hulls with minimum resistance to reduce the operational costs. Others have tried to design ships with a maximum cargo hold capacity without increasing their overall dimensions.

Several researchers have conducted various studies to optimise ship design. One study successfully increased the cargo capacity of tankers by 2.0% and bulk carriers by 1.94% using the Parametric Inner Shell Optimization Method (PISOM) [1]. Another study reduced the total and residual resistance coefficients by 2.4% and 6.8%, respectively, using Sequential Quadratic Programming (SQP) [2]. A combination of dynamic programming and a genetic algorithm was used to solve voyage planning in three dimensions, achieving an average fuel saving and emission reduction of 3.4% on a medium-size chemical tanker [3]. A CFD-based adjoint solver tool for modifying the hull form of a trimaran ship is presented, resulting in a 6.67% reduction in total resistance [4]. Multi-objective optimization design for composite panels of the superstructure in large passenger ships is performed using the Neighborhood Cultivation Genetic Algorithm (NCGA), with structural mass reduced by 4.1% and ultimate strength increased by 9.2% [5]. A route for a container ship was optimized using Dijkstra's algorithm, resulting in a fuel consumption decrease of around 6 tons and total costs that were 4.76% less than those of the great circle arc path [6]. A Japan Bulk Carrier (JBC) was optimized using the Dung Beetle Optimizer algorithm which resulting in a 4.7% decrease in resistance [7]. The optimization of the ship structure reduced the steel weight of OSV vessels by 121.9 tonnes (42.4%) using the blind search method [8]. The optimization of the Sectional Area of Curve (SAC) and the cross-sectional shape of the design load waterline (DLWL) reduced wave-making resistance by 13.2% and added resistance by 13.8% on bulk carriers, as determined by a study using Particle Swarm Optimization (PSO) [9]. Another study found that the production costs and construction weight of chemical tankers could be reduced by 3% and 2.18%, respectively, based on Common Structural Rules (CSR) [10]. Another study produced an optimal structural layout and scantling configuration using a semi-automatic design method with VBA [11]. A multi-fidelity deep neural network (MFDNN)-based framework is proposed to

improve hull form optimization by combining high- and low-fidelity data, achieving enhanced computational efficiency and accuracy while reducing resistance [12]. A data-driven hull shape optimization pipeline using reduced-order models, dynamic mode decomposition, and machine learning is developed to efficiently minimize ship drag, enabling genetic algorithm-based optimization with reduced computational cost [13]. A nonlinear programming-based hull form optimization method using B-spline parameters is developed to minimize total resistance by considering both wave-making and viscous effects and is validated through experimental testing on an improved Series60 model [14]. Another study successfully reduced the structural profile cross-sectional area by 4,425% and the ship's VCG by 1,267% using the Dominated Artificial Bee Colony (D-ABC) algorithm [15]. Recently, the design of a small coastal tanker was successfully optimized to increase its cargo capacity by 1.98% [16].

Tankers have become the backbone of the global economy by transporting the world's most widely used energy source: oil. By 2024, tankers accounted for 28.3% of the total deadweight (DWT) of commercial vessels worldwide [17]. Oil tankers are designed to transport crude or refined oil in bulk. They differ from other types of cargo vessel, such as bulk carriers, container ships and general cargo ships. They have no large hatch openings, only have one deck in their cargo hold area and double bottom and double side (wing tank) structures. At the intersection of these structures, in the inner bilge area, there is a sloped hopper structure.

The double bottom, double side, and hopper structures must comply with MARPOL 73/78 regulations, which stipulate that there must be a space or clearance between the ship's hull and the cargo oil tanks. This space is intended to prevent oil spills when the hull is damaged. However, these structures significantly reduce the volume of the cargo hold.

Despite extensive research on ship design optimization, most studies have focused on improving hydrodynamic performance, structural efficiency, routing, or material selection. Only a limited number of studies have addressed the optimization of cargo hold design. For example, previous approaches, such as Parametric Inner Shell Optimization Method (PISOM), have demonstrated improvements in cargo hold capacity. However, they generally retain conventional hopper configurations and do not explore alternative geometrical transformations of the inner bilge design. Therefore, the objective of this research is to explore the possibility of optimizing cargo hold volume by converting the sloped hopper design into a rounded inner bilge.

## 2. Method

### 2.1. Basic Theory

#### 2.1.1. MARPOL 73/78

MARPOL 73/78 is an international convention that addresses the prevention of pollution at sea caused by ship operations or accidents [18]. According to MARPOL Annex 1 Regulation 19, oil tankers over 600 DWT and built after 6 July 1996 must have wing tank and double bottom structures. A wing tank or double side tank is a tank or compartment structure that separates the cargo oil tank from the side shell of the ship, extending from the inner bottom to the main deck. According to Regulation 19.3.1, the width of the wing tanks ( $w$ ) can be calculated using formula (1), where DWT is the ship's deadweight while the value of  $w$  being limited to the range  $1 \leq w \leq 2$  m. A double bottom is a tank or compartment located at the bottom of the ship that separates the cargo oil tank from the ship's bottom. The height of the double bottom ( $h$ ) is determined using formula (2) with a value limit of  $1 \leq h \leq 2$  m where  $B$  is the ship's breadth, based on Regulation 19.3.2 [19]. The value of  $h$  and  $w$  is called minimum clearance.

$$w = 0.5 + DWT/20000 \text{ (m)} \quad (1)$$

$$h = B/15 \text{ (m)} \quad (2)$$

The double bottom and double side structures are intersected at the bilge area. The values of  $w$  and  $h$  on tankers can vary, resulting in changes to the minimum clearance of bilge area. According to Regulation 19.3.3, the minimum clearance between the hull shell and the cargo tanks in the bilge area must be  $h$  up to a height of  $1.5h$ , measured from the baseline. Above this height, the clearance must be  $w$ , as illustrated in Figure 1 [19].

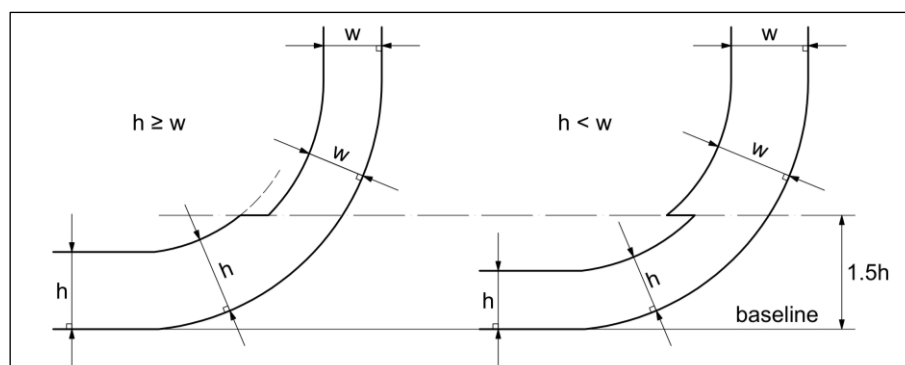


Figure 1. The Minimum Clearance between hull shell and cargo tank

### 2.1.2. B-Spline and Bézier Curve

A B-spline is a mathematical function used in numerical and computer analysis to create smooth curves and surfaces. A B-spline curve consists of several polynomial segments [20]. The main components of a B-spline are control points, knots and degrees. Control points determine the shape of the B-spline, while knots are the points at which the polynomial curves meet. The degrees affect the flexibility or rigidity of the curve because they determine the shape of the polynomial. B-splines and their advanced form, NURBS (Non-Uniform Rational B-Splines), are the standard technology used to create, represent, and manipulate complex freeform surfaces in computer-aided design (CAD) and computer-aided manufacturing (CAM) systems.

A B-spline is a generalization of a Bézier curve. A B-spline without internal knots is a Bézier curve [21]. For example, a B-spline with three control points without internal knots is created using a Bézier curve function. A Bézier curve is formed using only a single polynomial equation, so there are no knots, as shown in Figure 2 [22].

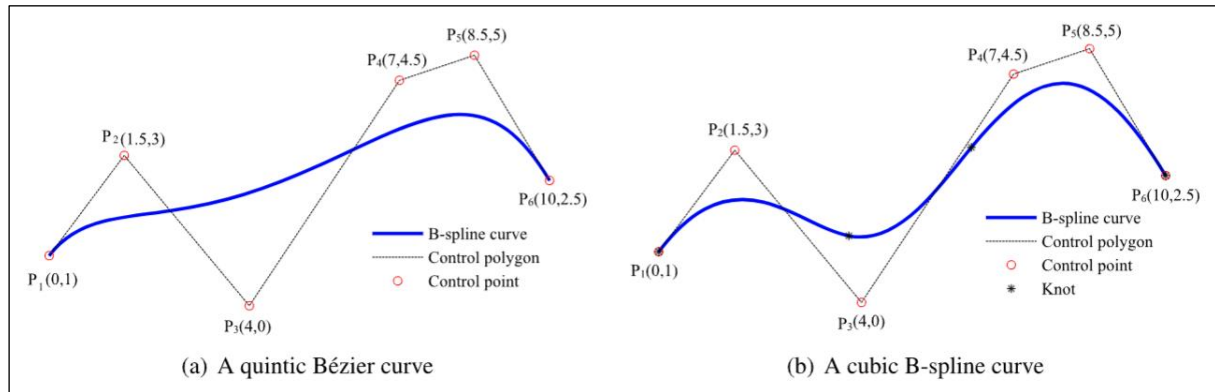


Figure 2. The Difference between a Bézier Curve and a B-Spline Curve [22]

A Bézier curve is formed using the Bernstein polynomial equation, which is why it is also known as the Bernstein-Bézier curve. A Bézier curve always passes through the first and second control points and always lies within the area connecting the remaining control points. One advantage of the Bézier curve is that its shape remains unchanged when all the control points undergo translation or rotation. However, yet changes to one control point will alter the shape of the entire curve. Bézier curve is defined by equation (3), while the Bernstein polynomial equation is given by equation (4) [23], [24]. This equation serves as the basis for generating the rounded inner bilge.

$$C(t) = \sum_{i=0}^n P_i B_{i,n}(t), \quad t \in [0,1] \quad (3)$$

$$B_{i,n}(t) = \binom{n}{i} t^i (1-t)^{n-i} \quad (4)$$

where,

- $C(t)$  = Bézier curve equation
- $P_i$  = control point coordinates (e.g.  $x_i, y_i$ )
- $B_{i,n}(t)$  = Bernstein polynomials
- $(n-1)$  = number of control point

### 2.1.3. Rounded Inner Bilge

This research will explore the use of a rounded inner bilge to replace the conventional sloped hopper in tanker design. This design will increase the cargo oil tank's volume. Many CAD software programs use B-splines to generate surfaces. Therefore, the inner bilge design will be generated using a Bézier curve which is a B-spline without internal knots. Bézier curve is a polynomial curve, meaning that the generated arc does not have a measurable radius, unlike a circular arc. Therefore, the control points of the Bézier curve must be placed precisely to ensure that the resulting curve resembles a circular arc. To achieve this, the three control points of the Bézier curve must form a symmetrical pattern, as shown in Figure 3. The inner bilge is represented by the red curve and the three control points are represented by the three red dots. This only applies when the arc angle resulting from this process is no greater than  $90^\circ$  [25]. The location of the third control point ( $y_3, z_3$ ) can be found using the circle equation and trigonometric formulas.

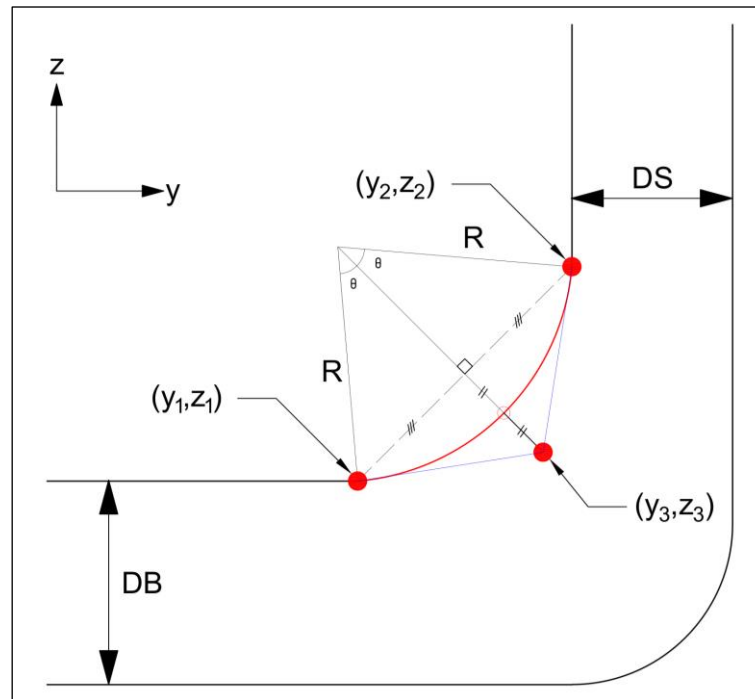


Figure 3. Inner bilge design formed using Bézier curve

#### 2.1.4. Grid Search Optimization Method

Nonlinear multivariable problems can be solved using various optimization methods, one of which is the grid search method. This method involves creating a grid with axes representing the variables. Each coordinate point on the grid is then examined against the objective function to find the maximum or minimum value of the problem [26]. For example, if the objective function is  $f(x_1, x_2)$  and the value interval of each variable is 1 to 4, as shown in Figure 4, then the number of coordinate points that must be examined is  $2^4 = 16$ . The more variables in the objective function, the more coordinate points that need to be examined. If the objective function has three variables, each with a value interval of 1 to 10, then the number of coordinate points to be examined is  $3^{10} = 59,049$ . The grid resolution depends on the selected step size, which determines the number of coordinate points evaluated. A smaller step size yields more accurate results, but it significantly increases the computational time. Unlike any heuristic method, this method can achieve the exact optimum result, but it takes a long time to obtain accurate results. Nevertheless, this method can be a good starting point for multivariable optimization problems, both constrained and unconstrained.

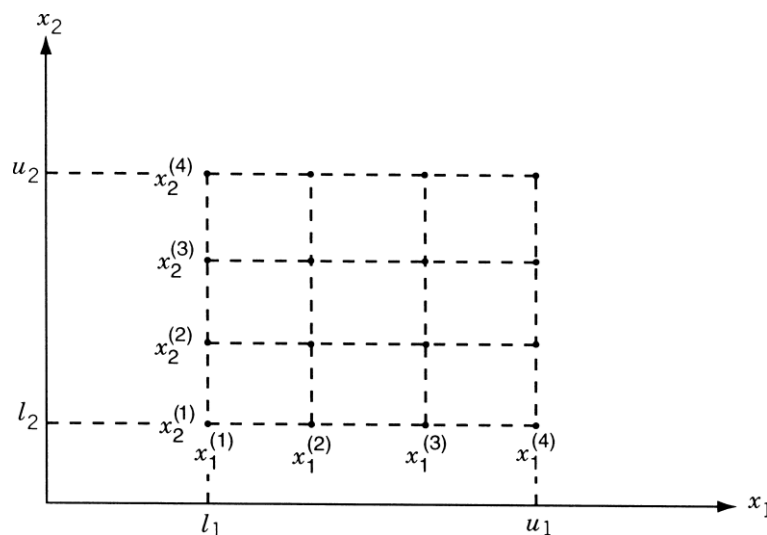


Figure 4. Grid Search Optimization Method

## 2.2. Data Collection and Ship Modelling

A tanker design model is generated using ship-modelling software based on the existing ship data. The data collected includes lines plan, general arrangement, construction profile, midship section, and stability booklet. The ship hull is generated using B-spline surfaces based on the lines plan, ensuring that its shape is as similar as possible to the existing ship. The general arrangement, construction profile and midship section are used for modelling the cargo oil tanks, while the stability booklet provides information about load distribution of the ship.

The ship design modelling is carried out using a sample vessel provided in the ship-modelling software, specifically a merchant ship model. The principal dimensions of this model are then adjusted to match those of the existing ship. However, this initial process may not accurately represent the existing ship. Therefore, further adjustments to the hull form are required by modifying the positions of the control points. These control points are iteratively adjusted until the lines plan and hydrostatic characteristics of the model comply with those of the existing ship. The model created is then validated by comparing its hydrostatic data with the existing data ensuring that the deviations remain within an acceptable tolerance.

This research will explore the use of a rounded inner bilge to replace the conventional sloped hopper in tanker design. This design will increase the cargo oil tank's volume. Many CAD software programs use B-splines to generate surfaces. Therefore, the inner bilge design will be generated using a Bézier curve which is a B-spline without internal knots. Bézier curve is a polynomial curve, meaning that the generated arc does not have a measurable radius, unlike a circular arc. Therefore, the control points of the Bézier curve must be placed precisely to ensure that the resulting curve resembles a circular arc. To achieve this, the three control points of the Bézier curve must form a symmetrical pattern, as shown in Figure 3. The inner bilge is represented by the red curve and the three control points are represented by the three red dots. This only applies when the arc angle resulting from this process is no greater than  $90^\circ$  [25]. The location of the third control point  $(y_3, z_3)$  can be found using the circle equation and trigonometric formulas.

## 2.3. Inner Bilge Optimization

### 2.3.1. Design Variables

Design variables are modified to minimize or maximize the objective function while satisfying the constraints. The variables in this research are the inner bilge radius ( $R$ ) and the location of two cargo landing points  $[(y_1, z_1) \& (y_2, z_2)]$  at every knuckle along the ship's cargo oil tank. Figure 5 shows the variables at one of the knuckle points in the ship's cargo oil tank. These variables will be varied, then the combination of variables that produces the most optimum objective function value will be selected as the optimum solution. The cargo landing point at the double bottom will be varied by shifting its coordinate transversely from initial position toward the double side. The cargo landing point at the double side will be varied by shifting its coordinate vertically from initial position toward the double bottom. Meanwhile the inner bilge will be varied by changing the radius from the minimum feasible value to the maximum allowable value.

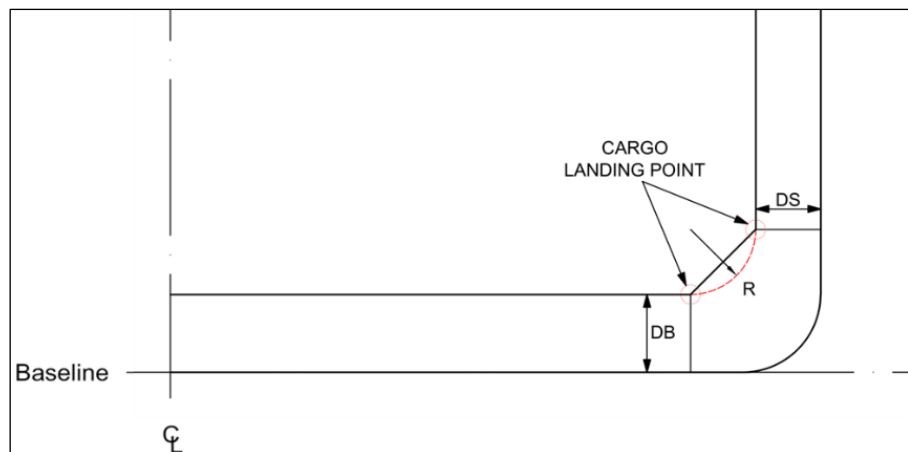


Figure 5. Illustration of the design variables at any cargo oil tank knuckle

In this research, there are several parameters that need to be considered, namely the height of the cargo landing point on the double bottom (DB) and the width of the cargo landing point on the double side (DS) which remain unchanged. The shape of the inner bilge shall not exceed the height of the double bottom and the width of the double side as shown in Figure 6.

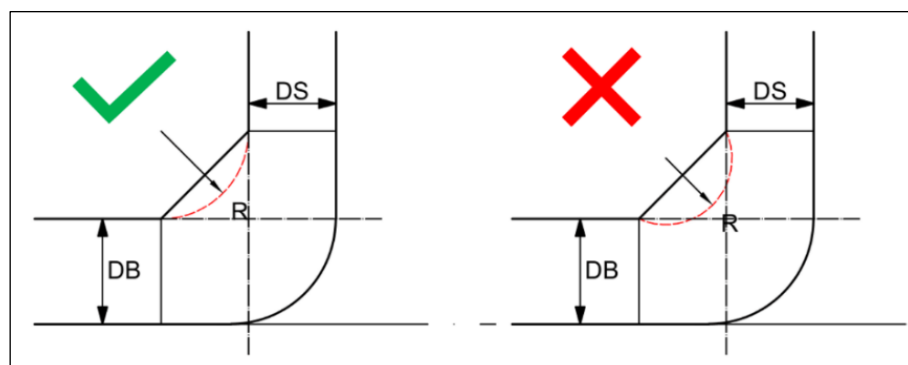


Figure 6. The desired shape of inner bilge

2.3.2. Objective Function

The objective function of this research is to maximize the volume of tanker cargo oil tank. The volume of the cargo oil tank increases if its cross-sectional area increases. Therefore, the objective function should focus on maximizing the cross-sectional area of the cargo oil tank at every knuckle. The equation to obtain the volume of the cargo oil tank is defined by formula (5), whereas the equation to obtain the cross-sectional area is given by equation (6) as illustrated by Figure 7.

$$V_{CH} = \int_0^{l_{CH}} A_{CH} dx \tag{5}$$

Cross sectional area = 2 · (Area of rectangle – Area of triangle + Area of segment)

$$A_{CH} = 2 \cdot \left[ ((H - z_1) \cdot y_2) - \left( \frac{1}{2} (z_2 - z_1) \cdot (y_2 - y_1) \right) + \left( \left( \frac{\theta}{360^\circ} \pi R^2 \right) - \left( \frac{1}{2} R^2 \sin \theta \right) \right) \right] \tag{6}$$

where  $\theta$  is obtained from equation (7) from cosine equation.

$$\cos \theta = \frac{R^2 + R^2 - ((y_2 - y_1)^2 + (z_2 - z_1)^2)}{2 \cdot R \cdot R} \tag{7}$$

$$\theta = \arccos \left( \frac{2R^2 - (y_2 - y_1)^2 - (z_2 - z_1)^2}{2R^2} \right)$$

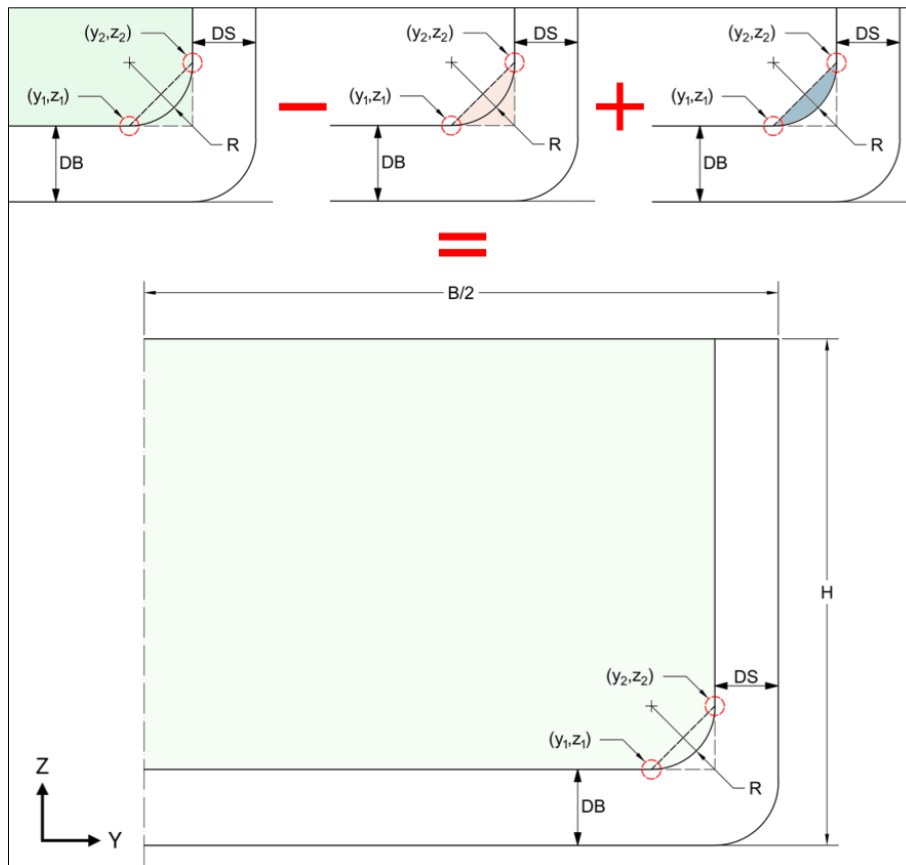


Figure 7. The illustration of calculating cross-sectional area

2.3.3. Constraints

Constraints are values that must be satisfied during the optimization process. In this research, the constraints are regulations governing clearance, stability, freeboard, still water bending moment (SWBM) and still water shear force (SWSF). The minimum clearance value is regulated in MARPOL Regulation 19.3, as well as in CSR Part 1 Chapter 2 Section 3. The constraints relating to stability and freeboard are regulated, respectively, in the IS Code 2008 Part A Chapter 2 and the International Convention on Load Lines (ICLL) 1966. CSR also regulates the maximum and minimum SWBM and SWSF for ships. In addition to these regulatory constraints, there are also geometric constraints to ensure that the shape of the inner bilge remains within reasonable shape.

The first geometric constraint relates to the combination of the cargo landing point coordinates. The cargo landing point at the double bottom ( $y_1, z_1$ ) must not be shifted transversely passing the transverse coordinate of the cargo landing point at

the double side ( $y_2, z_2$ ). Similarly, the cargo landing point at the double side ( $y_2, z_2$ ) must not be shifted vertically by passing the vertical coordinate of the cargo landing point at the double bottom ( $y_1, z_1$ ). This constraint is shown by Figure 8 (a).

The second geometric constraint is the maximum number of variations in the inner bilge radius. As shown in Figure 6, the inner bilge shall not exceed the height of the double bottom or the width of the double side. Furthermore, Figure 8 (b) shows that there are an infinite number of variations for the inner bilge radius, which requires a limit to be set. While a larger radius limit produces more variation, it also makes the shipbuilding process more complex.F8

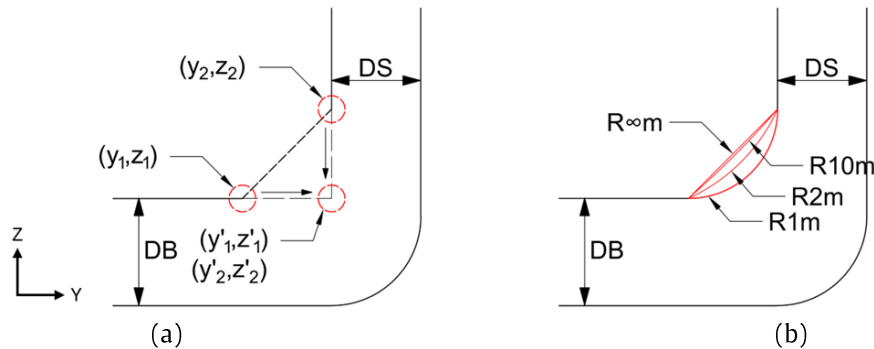


Figure 8. The geometric constraints of inner bilge optimization

## 2.4. Optimization Method

The optimization is performed using the grid search method, where each coordinate point of the variable combination must be examined. To calculate the total combination of all variables, the number of variations of each variable must be multiplied together. Equation (8) shows that the total combination can be obtained by multiplying the number of variations of the two cargo landing points and the number of variations of the inner bilge radius.

$$t = \sum_{i=1}^n \left( \frac{y_{2,i} - y_{1,i}}{m} \right) \cdot \left( \frac{z_{2,i} - z_{1,i}}{m} \right) \cdot \left( \frac{R_{max,i} - R_{min,i}}{m} \right) \quad (8)$$

where,  $t$  is the total number of combinations,  $i$  is the knuckle point, and  $m$  is the precision or step increment.

Every combination of variables shall not violate the constraint of minimum clearance based on MARPOL 73/78. To examine the clearance of the inner bilge, the arc of the inner bilge and the outer hull line are broken into some points, as shown in Figure 9. The inner bilge points are obtained from the Bézier curve from equation (3), while the outer hull points are obtained from ship-modelling-software. The distance between all the inner bilge points and all the outer hull points are measured. If the distance is less than the minimum clearance value, then the variation will be passed over.

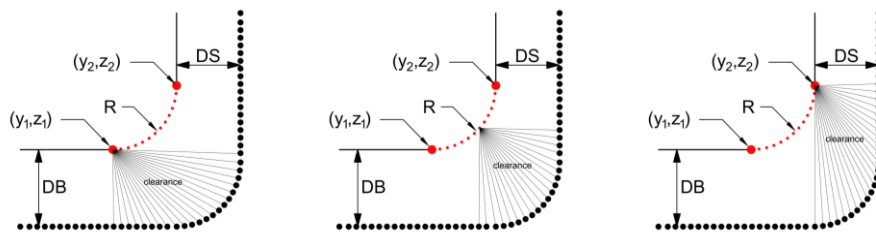


Figure 9. The illustration of clearance examination

The flowchart of clearance examination and the optimization process is shown in Figure 10. Following is the detail of the process.

- i. Collect the data of cargo landing point coordinates at the double bottom and double side at every knuckle along the cargo oil tank ( $(y_1, z_1)$  and  $(y_2, z_2)$ ). Then calculate the minimum clearance value  $h$  and  $w$  according to equation (1) and (2).
- ii. Examine the clearance for cargo landing point at the double bottom. If the clearance is greater than the minimum value of  $h$ , then the optimization process can be continued. Otherwise, there is no more variation that can satisfy the clearance constraint, so the examination can be terminated and move to process (iv).
- iii. Examine the clearance for cargo landing point at the double side. If the clearance is greater than the minimum value of  $w$ , then the optimization process can be continued. Otherwise, there is no more variation that can satisfy the clearance constraint. Therefore, the examination can be terminated, the coordinate will be back to initial value, and the process will move back to process (ii).
- iv. Pick the smallest possible radius to generate the inner bilge points based on equation (3). The distance between every inner bilge point and every outer hull point is measured. If the height of the inner bilge point is less than  $1.5h$ , then the clearance shall not be less than the minimum value  $h$ . If the height of the inner bilge point is more than  $1.5h$ , then the clearance shall not be less than the minimum value  $w$ . If the height of the inner bilge point is equal to  $1.5h$ , then the clearance shall not be less than the greatest value between  $h$  and  $w$ . When the

examination shows that clearance is less than the minimum value, then the variation of the inner bilge radius will be added by  $m$  until it satisfies the minimum value.

- v. If every inner bilge point satisfies the minimum clearance value, then the cross-sectional area of cargo oil tank will be calculated and saved. Furthermore, the variation of cargo landing points is added by  $m$  and the process will move back to (iii).
- vi. If there is no more possible combination that satisfies the minimum clearance, then combination resulting the maximum cross-sectional area of cargo oil tank will be selected.

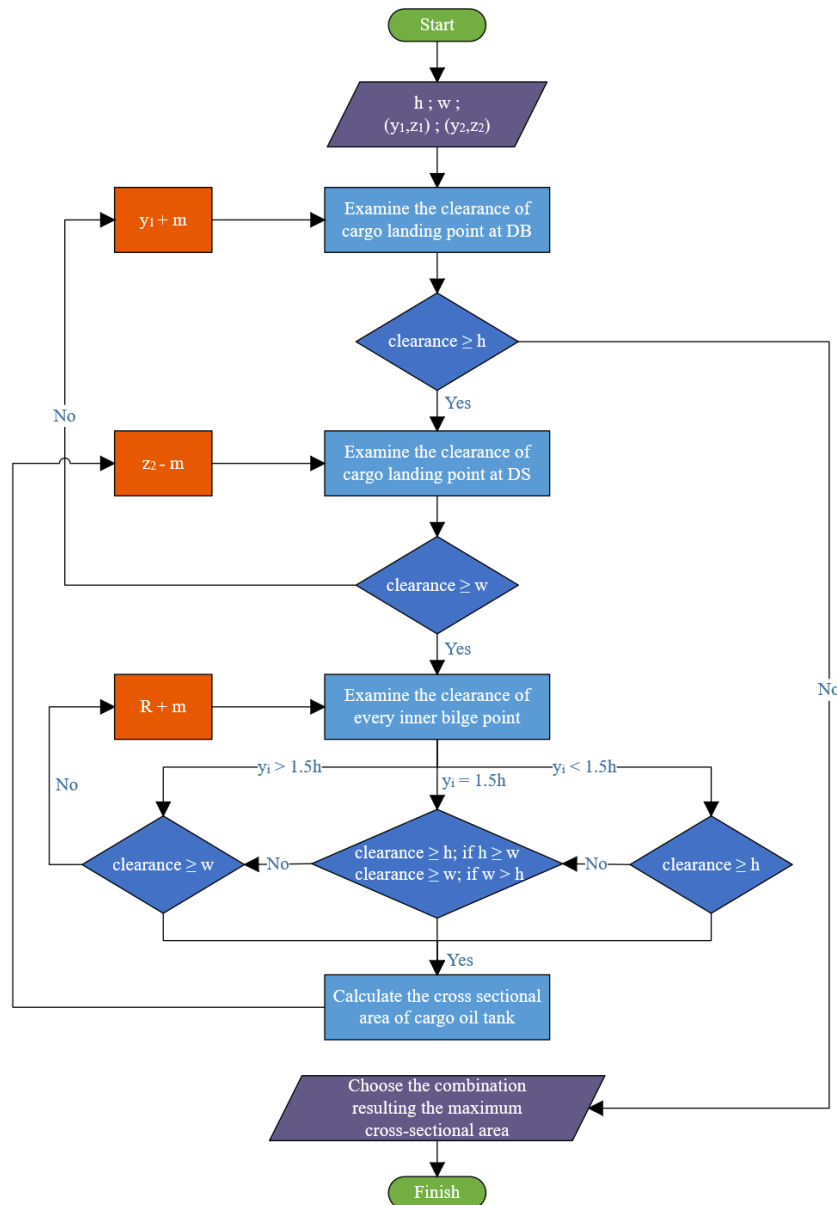


Figure 10. The flowchart of optimization process

## 2.5. Program Development

The programming language used in this research is Visual Basic for Application (VBA). VBA is a programming language developed by Microsoft and used to control Microsoft Office Excel [27]. It has proven to be an effective and efficient tool for handling repetitive tasks [28]. It can also be used to automate other software, including ship-modelling software. Figure 11 shows the flowchart of the inner bilge optimization program.

The program's input is data of the existing ship, consisting of lines plan, general arrangement, midship section, construction profile and stability booklet. This data is used to generate a model of ship and tanks manually in ship-modelling software. Some of the data (e.g. main dimensions, knuckle points' longitudinal coordinates, and ship deadweight) is also be used as initial input at the preprocessor stage, prior to the regulation checking process.

The program will command ship-modelling software to perform the regulation checking, starting with calculating of the tank volume and running the freeboard, stability, and longitudinal strength analysis. The result of the regulation checking of the existing ship will be recorded for comparison at the end of the optimization process.

The program will import the existing ship data from ship-modelling software. This data includes the coordinates of each cargo landing point and the outer hull points at each knuckle point. This data will be used in the inner bilge optimization

process. The results of the optimization process will then be exported to ship-modelling software. The ship model and tanks design will then be updated according to the new optimized data.

The next stage is to perform regulation checking on the optimized ship design. The freeboard, stability, and longitudinal strength will be analyzed. If any results fail to meet the minimum criteria, the program will perform the inner bilge optimization by taking the next possible solution until the minimum criteria are met. Only then will the actual optimized tank volume be calculated. The results of the optimized regulation checking and volume calculation will be recorded alongside the existing ship data.

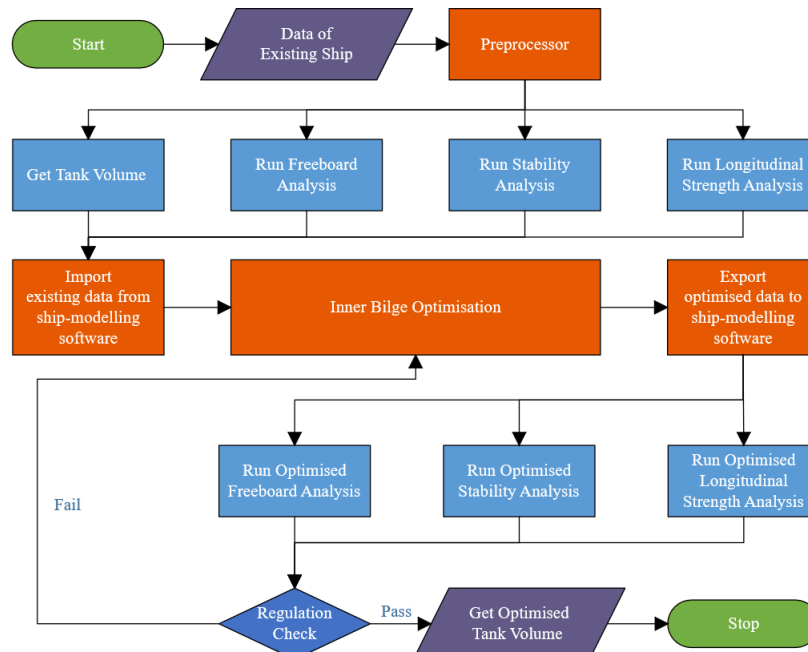


Figure 11. The flowchart of inner bilge optimization program

## 2.6. Regulation Checking

The ship design underwent regulation checking related to freeboard, stability, and longitudinal strength before and after optimization. All calculations to obtain stability, hydrostatic and longitudinal strength data were performed using ship modelling software. Ship's freeboard, stability, and longitudinal strength checks are performed on each loading condition both before and after optimization. The stability criteria that must be met are specified in the IS Code 2008 Part A Chapter 2. Freeboard checks are performed by obtaining the ship's actual draft. This data is then compared with the maximum criteria based on ICLL 1966. The maximum draft criteria can be obtained by subtracting the height of the ship with the minimum freeboard criteria based on ICLL 1966. The longitudinal strength criteria examined are SWBM and SWSF. The moment and shear data obtained from the analysis are then compared with the maximum criteria from CSR. Bending moments with positive values in the ship will be compared with the maximum hogging criteria, while those with negative values will be compared with the minimum sagging criteria.

## 2.7. Existing and Optimized Design Comparison

The final stage in this research is to compare the existing design with the optimized design. Items to be compared include changes in cargo oil tank volume, ship hydrostatic data, stability data and longitudinal strength data. This stage determines the extent to which inner bilge optimization influences a ship's design.

## 3. Results and Discussion

### 3.1. Existing Ship Data

The research focuses on a 30,000 DWT product oil tanker, with the principal dimensions outlined in Table 1.

Dimensions	Value (m)
Length overall (Loa)	180.00
Length between perpendiculars (Lpp)	173.00
Breadth (B <sub>mld</sub> )	30.50
Depth (H <sub>mld</sub> )	15.90
Designed draft (T <sub>mld</sub> )	9.00
Summer load draft	9.016

### 3.2. Ship Model

The ship hull and cargo oil tank were generated using a ship-modelling software, as shown in Figure 12. The difference in moulded volume displacement between the ship model and the real ship is about 0.048%. The existing height of the double bottom of the cargo oil tank is 2.05 m at the midship, while the width of the double side is 2.00 m at the midship. The cargo oil tank consists of six knuckle points and consists of 14 separate tanks with 37 different loading conditions.

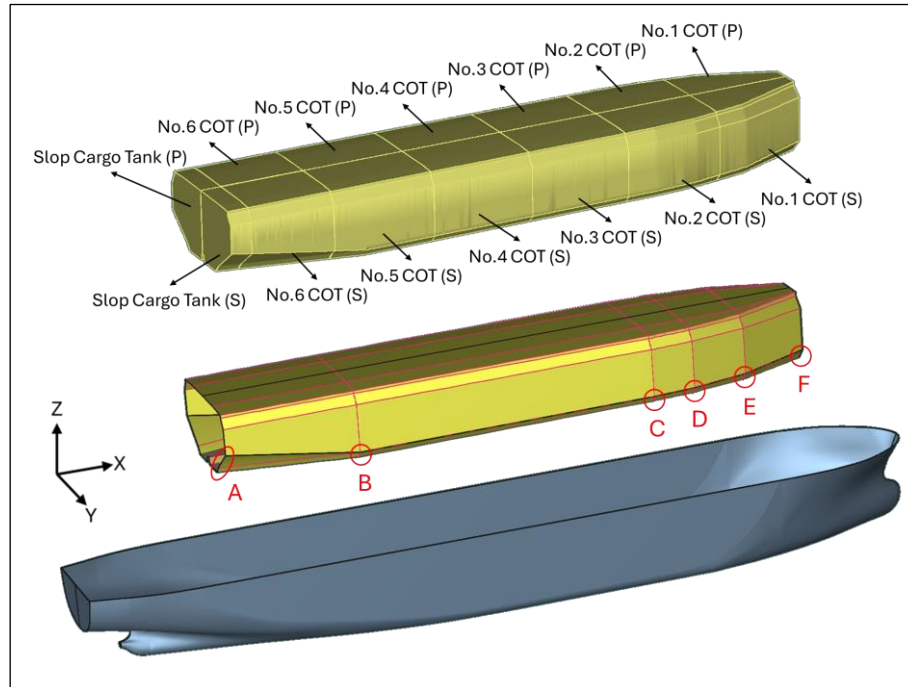


Figure 12. Existing ship and cargo oil tank model

### 3.3. Optimized Design

In this research, the first design variable was the cargo landing point on the double bottom. The point was shifted by 0.05 m increments in a transverse direction until the minimum clearance was met. Similarly, the second design variable, the cargo landing point on the double side was shifted vertically by 0.05 m increments. Meanwhile, the inner bilge radius design variable was varied in increments of 0.1 m until the minimum clearance was met. Table 2 shows the optimization results for the cargo landing point and the inner bilge radius at each knuckle point. This data represents the combination resulting in the largest cargo hold cross-sectional area. Figures 13 to 15 show the inner bilge design results after optimization. Figure 16 illustrates the resulting optimal combination obtained using the grid search optimization method.

The combination of cargo hold section area increases from knuckle point A to point F would result in cargo hold volume increase. The increase in volume then should be further analyzed to make sure that the ship with optimized cargo hold design still complies to the regulation requirements.

Table 2. Design Variables Optimization Results

No.	Cargo Landing Point	X (m)	Y (m)		Z (m)		Radius (m)
			Existing Ship	Optimized	Existing Ship	Optimized	
1	A1	37.05	5.80	6.20	2.05	2.05	13.10
	A2	37.05	13.25	13.25	8.00	7.10	
2	B1	64.80	12.00	12.40	2.05	2.05	1.10
	B2	64.80	13.25	13.25	3.45	2.65	
3	C1	127.80	12.00	13.10	2.05	2.05	2.20
	C2	127.80	13.25	13.25	3.45	2.85	
4	D1	136.80	11.50	12.15	2.05	2.05	1.70
	D2	136.80	12.80	12.80	3.51	3.256	
5	E1	148.80	9.40	9.40	2.05	2.05	2.70
	E2	148.80	10.93	10.93	3.74	3.644	
6	F1	163.80	3.15	3.30	2.05	2.05	4.20
	F2	163.80	5.30	5.30	4.46	3.608	

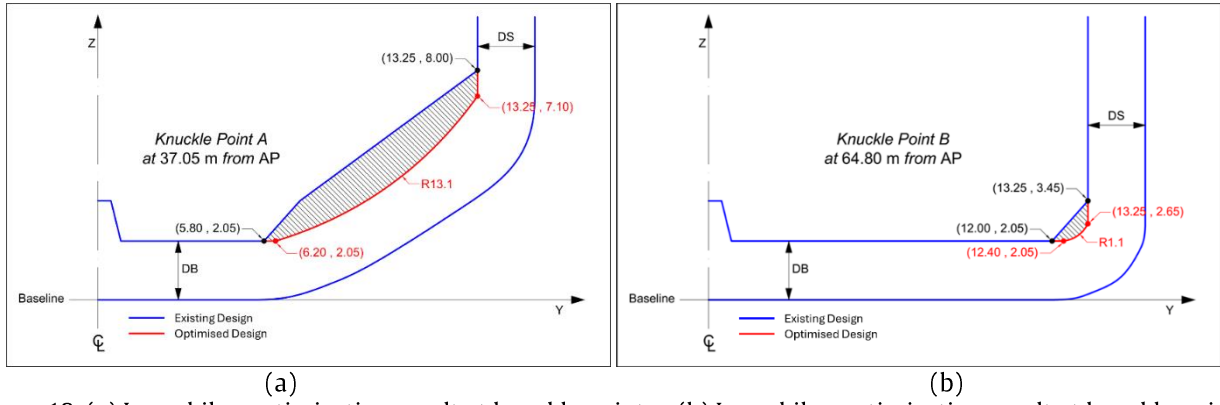


Figure 13. (a) Inner bilge optimization result at knuckle point a; (b) Inner bilge optimization result at knuckle point b

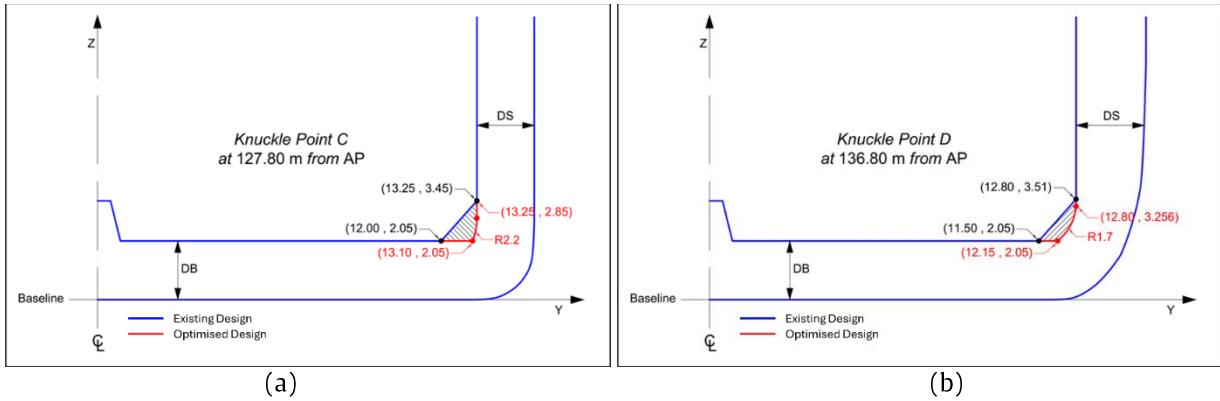


Figure 14. (a) Inner bilge optimization result at knuckle point c; (b) Inner bilge optimization result at knuckle point d

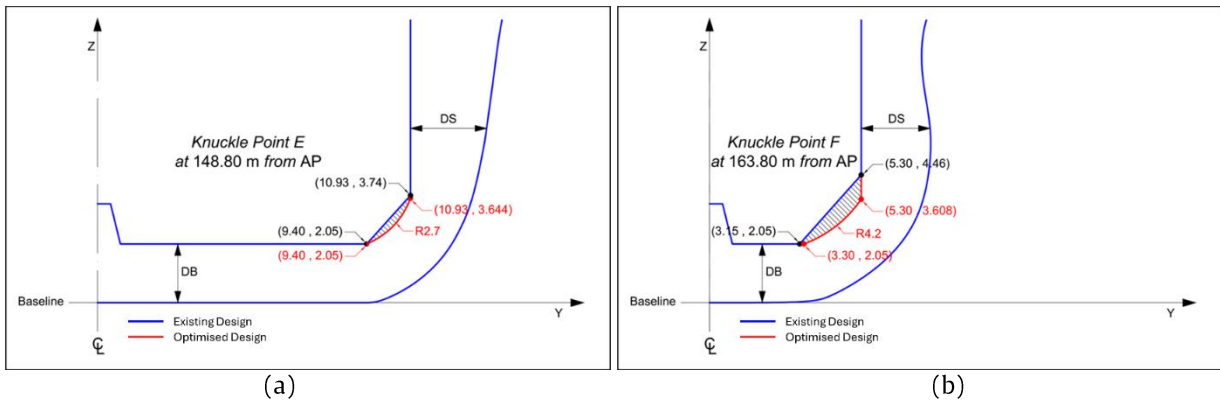


Figure 15. (a) Inner bilge optimization result at knuckle point e; (b) Inner bilge optimization result at knuckle point f

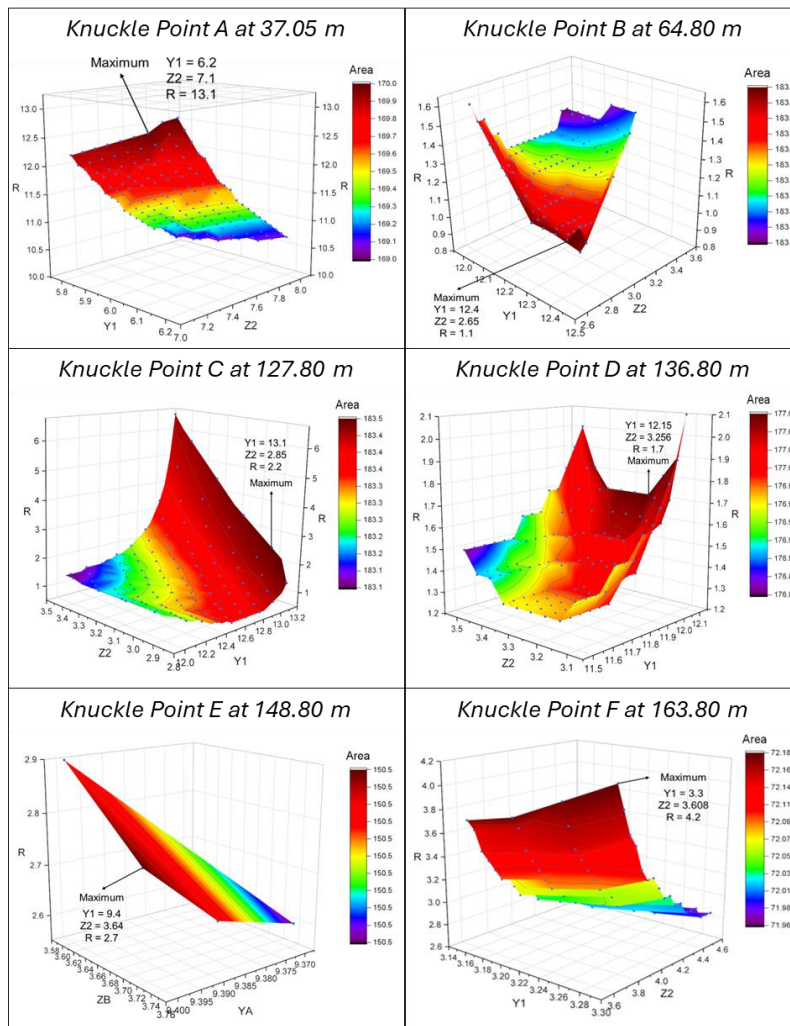


Figure 16. Results of grid search optimization method

### 3.4. Regulation Checking

The optimization process results in an increase in cargo oil tank volume while the hull design remains unchanged. Consequently, the draft increases, and therefore the freeboard must be reassessed to ensure compliance with regulatory requirements. Based on ICLL 1966, the minimum freeboard for a tanker with principal dimension listed in Table 1 is 4.187 m making the maximum draft 11.713 m. According to the freeboard analysis, all the 37 loading conditions passed the criteria. The Full Load Arrival Condition for Short Voyage conditions have the highest increase in draft, at around 0.057 m or 0.640%.

The increase in cargo oil tank volume also affects the ship's centre of gravity and load distribution. Specifically, the increase in cargo leads to a slight lowering of the centre of gravity, which in turn improves the ship's stability. According to the stability analysis, all the criteria required by IS Code 2008 are met for all loading conditions. As shown in Table 3, the additional cargo oil tank volume causes the stability criteria to have a higher value than that of the existing ship. The SWBM and SWSF values for the ship also change slightly due to the additional cargo oil tank volume, as shown in Table 4.

Table 3. Intact Stability Analysis at Full Load Arrival Condition for Short Voyage Condition

Criteria	Required Value	Existing Ship	Optimized Ship
Area under GZ curve between heel angles of 0 to 30 degrees shall not be less than (m.rad)	0.055	0.642	0.645
Area under GZ curve between heel angles of 0 to 40 degrees shall not be less than (m.rad)	0.090	1.138	1.143
Area under GZ curve between heel angles of 30 to 40 degrees shall not be less than (m.rad)	0.030	0.496	0.498
The righting lever GZ shall be at least 0.2 m at an angle of heel equal to or greater than (m)	0.200	2.948	2.957
The maximum righting lever shall occur at an angle of heel not less than (degrees)	25.0	40.0	40.0
The initial metacentric height GM0 shall not be less than (m)	0.150	4.301	4.331

Table 4. SWBM and SWSF Analysis at Full Load Arrival Condition for Short Voyage Condition

Frame No.	Longitudinal Position (m)	Existing Ship SWSF (kiloton)	Optimized - Ship SWSF (kiloton)	Allowable SWSF (kiloton)	Existing Ship SWBM (kiloton.m)	Optimized - Ship SWBM (kiloton.m)	Allowable SWBM (kiloton.m)
55	40.8	-1.142	-1.184	-2.377	0.237	-1.476	-51.625
61	58.8	-0.554	-0.508	-2.887	-15.090	-16.530	-67.200
68	79.8	0.122	0.154	3.326	-19.342	-19.919	-67.200
75	100.8	0.742	0.759	3.326	-9.883	-9.960	-67.200
82	121.8	-0.395	-0.394	-2.887	-6.725	-6.632	-67.200
89	142.8	0.208	0.205	2.377	-7.926	-7.850	-17.359
96	163.8	0.336	0.338	2.377	-1.456	-1.463	-1.711

### 3.5. Existing and Optimized Design Comparison

The objective function of this research is to maximise the volume of the cargo oil tank. Based on the analysis, the cargo oil tank volume increased by 417.515 m<sup>3</sup> or 0.960%. Although this increase may appear modest, it is significant in tanker operations, as even small gains in cargo capacity can lead to higher revenue per voyage or allow for a reduction in principal dimensions while maintaining the same payload. Table 5 shows the extent of the increase in cargo oil tank volume in each compartment and Figure 17 illustrates the additional volume after optimization.

The magnitude of the volume increase is significantly governed by MARPOL clearance requirements, which restrict the extent to which the internal geometry can be modified. However, the proposed rounded inner bilge configuration introduces trade-offs in terms of fabrication and constructability during the shipbuilding process. The rounded inner bilge introduces greater complexity compared to the conventional sloped hopper, particularly in fabrication and assembly process. In the future, this design may become more feasible with advancements in fabrication technology and reductions in production costs.

Table 5. Cargo Oil Tank Volume After Optimization

Tank Name	Existing Volume (m <sup>3</sup> )	Optimized Volume (m <sup>3</sup> )	Additional Volume (m <sup>3</sup> )	Additional Volume (%)
No.1 COT (S)	2689.418	2705.610	16.192	0.602%
No.1 COT (P)	2690.579	2706.775	16.196	0.602%
No.2 COT (S)	3764.589	3780.352	15.763	0.419%
No.2 COT (P)	3775.420	3791.232	15.812	0.419%
No.3 COT (S)	3864.170	3880.527	16.357	0.423%
No.3 COT (P)	3866.015	3882.375	16.360	0.423%
No.4 COT (S)	3870.627	3886.040	15.413	0.398%
No.4 COT (P)	3868.782	3884.186	15.403	0.398%
No.5 COT (S)	3862.503	3882.357	19.854	0.514%
No.5 COT (P)	3866.863	3886.877	20.014	0.518%
No.6 COT (S)	2992.031	3078.561	86.530	2.892%
No.6 COT (P)	2991.681	3078.343	86.662	2.897%
Slop Cargo Tank (S)	692.026	730.675	38.649	5.585%
Slop Cargo Tank (P)	685.182	723.491	38.310	5.591%
<b>Total</b>	<b>43479.887</b>	<b>43897.401</b>	<b>417.515</b>	<b>0.960%</b>

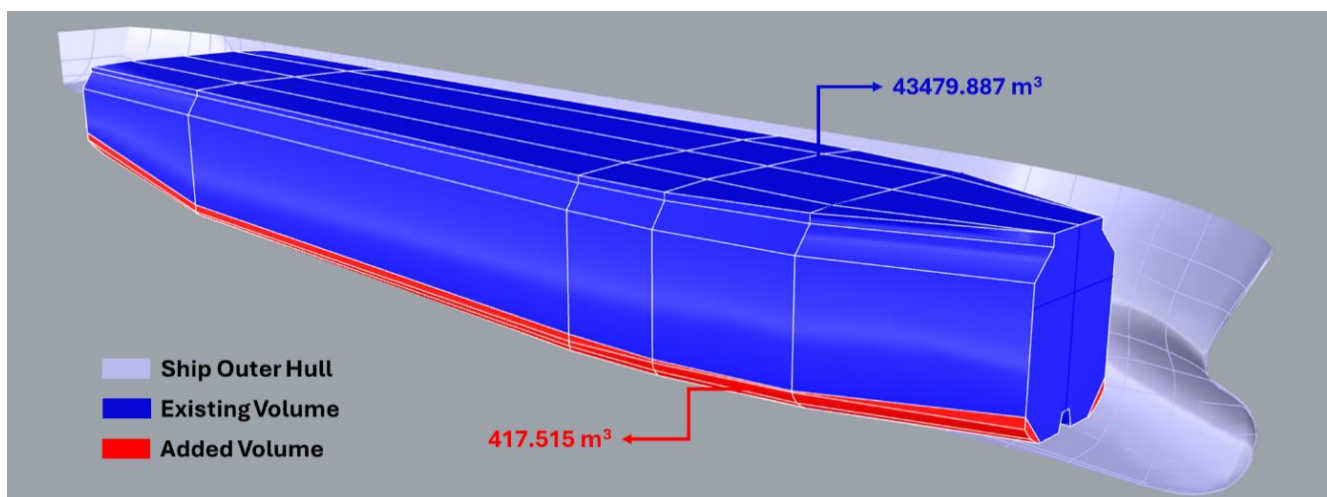


Figure 17. Added cargo oil tank volume 3D model

### 3.6. Length Reduction

Building a sister ship with the same payload but with an optimized cargo oil tank design configuration (inner bilge optimization) would reduce the length of the cargo oil tanks and the ship itself. This reduction in length can be achieved by dividing the additional cargo volume by the optimized cargo oil tank cross-sectional area at midship. The calculation results below show that the ship's length can be reduced by 1.122 meters along the parallel middle body.

Length reduction = (Added volume)/(Cargo oil tank cross-sectional area at midship)

$$l = \frac{417.515 \text{ m}^3}{372.202 \text{ m}^2} = 1.122 \text{ m}$$

The reduction in length implies that the plates and the longitudinal stiffeners within the cargo oil tank along the parallel middle body would be 1.122 meters shorter, resulting in lower material usage and reduced structural weight. This condition can provide practical advantages in shipbuilding, such as lower material costs and shorter construction time. However, the reduction in structural weight may also affect the actual stability of the completed ship, potentially leading to deviations from the existing design stability, freeboard, and longitudinal strength. Therefore, stability, freeboard, and longitudinal strength compliance are included as a constraint in the optimization process to ensure that both the optimized design and the reduced-length design achieve acceptable performance with minimal deviation while remaining within the required criteria.

## 4. Conclusion

The inner bilge optimization applied to an existing tanker ship design using a grid search method resulted in a new design with 417.515 m<sup>3</sup>, or 0.960% increase in cargo oil tank volume compared to the existing original design. This optimization affected several design parameters such as freeboard, stability and longitudinal strength, but still successfully comply to regulatory requirements. The inner bilge optimization applied to an existing tanker ship design using a grid search method resulted in a new design with an increase in cargo oil tank volume of 417.515 m<sup>3</sup>, or 0.960%, compared to the original design. This optimization affected several design parameters such as freeboard, stability and longitudinal strength, but still successfully comply to regulatory requirements. The increase in cargo oil tank volume can compensate for a reduction of up to 1.122 meters in the lengths of both the ship and the cargo oil tanks along the parallel middle body, which then could be used to build a sister ship with the same payload but more efficient cargo oil tank configuration. Nevertheless, as this study considers only a single tanker design and single optimization method, further study is required before applying these findings to develop new ship design and extending the optimization approach in this study to other ship types or configurations. Future studies should consider multiple optimization methods and tanker designs to evaluate the applicability and robustness of the optimization method by comparing the consistency of the result. In addition, for practical implementation in shipbuilding, further analysis for the hydrodynamic performance of the optimized design should be conducted by considering the overall weight and length reduction.

## Acknowledgements

The authors would like to appreciate the financial support from Department of Naval Architecture, Faculty of Marine Technology and the Institut Teknologi Sepuluh Nopember under project scheme of the Publication Writing and IPR Incentive Program (PPHKI) and the Strategic Research Grant (SRG) 2026 scheme (Contract No. 1078/PKS/ITS/2026).

## References

- [1] Y. Y. Yu, Y. Lin, M. Chen, and K. Li, "A New Method for Ship Inner Shell Optimization Based on Parametric Technique," *International Journal of Naval Architecture and Ocean Engineering*, vol. 7, no. 1, pp. 142–156, 2015, doi: <https://doi.org/10.1515/ijnaoe-2015-0011>.
- [2] J. H. Park, J. E. Choi, and H. H. Chun, "Hull-Form Optimization of KSUEZMAX to Enhance Resistance Performance," *International Journal of Naval Architecture and Ocean Engineering*, vol. 7, no. 1, pp. 100–114, 2015, doi: <https://doi.org/10.1515/ijnaoe-2015-0008>.
- [3] H. Wang, X. Lang, and W. Mao, "Voyage optimization combining genetic algorithm and dynamic programming for fuel/emissions reduction," *Transp. Res. D Transp. Environ.*, vol. 90, p. 102670, Jan. 2021, doi: <https://doi.org/10.1016/j.trd.2020.102670>.
- [4] A. Nazemian and P. Ghadimi, "Shape optimisation of trimaran ship hull using CFD-based simulation and adjoint solver," *Ships and Offshore Structures*, vol. 17, no. 2, pp. 359–373, Feb. 2022, doi: <https://doi.org/10.1080/17445302.2020.1827807>.
- [5] B. Liu, J. Jiang, and D. K. Kim, "Structural analysis and optimisation of GFRP sandwich panel with steel stiffeners in upper decks of large passenger ships," *Ships and Offshore Structures*, pp. 1–13, Mar. 2025, doi: <https://doi.org/10.1080/17445302.2025.2478367>.
- [6] N. Bahrami and S. M. Siadatmousavi, "Ship voyage optimisation considering environmental forces using the iterative Dijkstra's algorithm," *Ships and Offshore Structures*, vol. 19, no. 8, pp. 1173–1180, 2024, doi: <https://doi.org/10.1080/17445302.2023.2231200>.

- [7] Y. Wei, H. Zhang, D. Jiang, Y. Zhang, and S. Xiao, "Optimising ship principal dimensions with a Dung Beetle Optimizer and random forest proxy model," *Ships and Offshore Structures*, vol. 20, no. 11, pp. 1789–1800, Nov. 2025, doi: <https://doi.org/10.1080/17445302.2024.2397928>.
- [8] A. M. H. Elhewy, A. M. A. Hassan, and M. A. Ibrahim, "Weight Optimization of Offshore Supply Vessel Based on Structural Analysis Using Finite Element Method," *Alexandria Engineering Journal*, vol. 55, no. 2, pp. 1005–1015, 2016, doi: <https://doi.org/10.1016/j.aej.2016.02.032>.
- [9] J. W. Yu, C. M. Lee, I. Lee, and J. E. Choi, "Bow Hull-Form Optimization in Waves of a 66,000 DWT Bulk Carrier," *International Journal of Naval Architecture and Ocean Engineering*, vol. 9, no. 5, pp. 499–508, 2017, doi: <https://doi.org/10.1016/j.ijnaoe.2017.01.006>.
- [10] M. Sayebani, A. Mohammadrahimi, and H. K. Looyeh, "Weight and Cost Optimization of Midship Section Using Common Structural Rules," pp. 20–22, 2020.
- [11] M. Aguiari, M. Gaiotti, and C. M. Rizzo, "Ship Weight Reduction by Parametric Design of Hull Scantling," *Ocean Engineering*, vol. 263, no. August, p. 112370, 2022, doi: <https://doi.org/10.1016/j.oceaneng.2022.112370>.
- [12] Y. Wei, G. Pan, P. Paladaechanan, and D. Wan, "A novel hull form optimization framework based on multi-fidelity deep neural network," *Journal of Hydrodynamics*, vol. 37, no. 1, pp. 149–159, Feb. 2025, doi: <https://doi.org/10.1007/s42241-025-0007-4>.
- [13] N. Demo, G. Ortali, G. Gustin, G. Rozza, and G. Lavini, "An efficient computational framework for naval shape design and optimization problems by means of data-driven reduced order modeling techniques," *Bollettino dell'Unione Matematica Italiana*, vol. 14, no. 1, pp. 211–230, Mar. 2021, doi: <https://doi.org/10.1007/s40574-020-00263-4>.
- [14] B.-J. Zhang and Z.-X. Zhang, "Research on theoretical optimization and experimental verification of minimum resistance hull form based on Rankine source method," *International Journal of Naval Architecture and Ocean Engineering*, vol. 7, no. 5, pp. 785–794, Sep. 2015, doi: <https://doi.org/10.1515/ijnaoe-2015-0055>.
- [15] C. Jiang, S. Yang, P. Nie, and X. Xiang, "Multi-objective structural profile optimization of ships based on improved Artificial Bee Colony Algorithm and structural component library," *Ocean Engineering*, vol. 283, p. 115124, Sep. 2023, doi: <https://doi.org/10.1016/j.oceaneng.2023.115124>.
- [16] A. N. Yulianto, "Research on The Methodology of Hull Weight Reduction Considering The Variations of Compartment Arrangement and Ship Length for Small Coastal Tanker," Mokpo National University, 2023.
- [17] United Nations, *REVIEW OF MARITIME TRANSPORT: Navigating Maritime Chokepoints*. Geneva: UNITED NATIONS PUBLICATIONS, 2024.
- [18] H. A. Kurniawati, *Statutory Regulations*. Surabaya: Departemen Teknik Perkapalan Fakultas Teknologi Kelautan ITS, 2020.
- [19] IMO, *International Convention for the Prevention of Pollution from Ships (MARPOL)*. London, 1973.
- [20] G. Farin, "B-Spline Curves," *Curves and Surfaces for CAGD*, pp. 119–146, Jan. 2002, doi: <https://doi.org/10.1016/B978-155860737-8/50008-9>.
- [21] E. W. Weisstein, "B-Spline," MathWorld--A Wolfram Web Resource. Accessed: Jun. 22, 2024. [Online]. Available: <https://mathworld.wolfram.com/B-Spline.html>
- [22] D. T. T. Do and J. Lee, "An Automatically Connected Graph Representation Based on B-Splines for Structural Topology Optimization," *Structural and Multidisciplinary Optimization*, vol. 59, no. 6, pp. 2023–2040, Jun. 2019, doi: <https://doi.org/10.1007/s00158-018-2170-5>.
- [23] E. W. Weisstein, "Bézier Curve," MathWorld--A Wolfram Web Resource. Accessed: Jun. 23, 2024. [Online]. Available: <https://mathworld.wolfram.com/BezierCurve.html>
- [24] E. W. Weisstein, "Bernstein Polynomial," MathWorld--A Wolfram Web Resource. Accessed: Jun. 22, 2024. [Online]. Available: <https://mathworld.wolfram.com/BernsteinPolynomial.html>
- [25] A. Rababah, "The Best Uniform Quadratic Approximation of Circular Arcs with High Accuracy," *Open Mathematics*, vol. 14, no. 1, pp. 118–127, Mar. 2016, doi: <https://doi.org/10.1515/math-2016-0012>.
- [26] S. S. Rao, *Engineering Optimization: Theory and Practice*. New J: John Wiley & Sons, 2019. doi: 10.1002/9781119454816.
- [27] J. Walkenbach, *Excel VBA Programming for Dummies*, 2nd ed. Indiana: Wiley Publishing, 2010.
- [28] Office 365 et al., "Getting Started with VBA in Office." Accessed: Nov. 11, 2023. [Online]. Available: <https://learn.microsoft.com/en-us/office/vba/library-reference/concepts/getting-started-with-vba-in-office>.